

# Antidepressant effects of curcumin and HU-211 coencapsulated solid lipid nanoparticles against corticosterone-induced cellular and animal models of major depression

Xiaolie He\*  
Yanjing Zhu\*  
Mei Wang  
Guoxin Jing  
Rongrong Zhu  
Shilong Wang

Research Center for Translational Medicine at East Hospital, School of Life Science and Technology, Tongji University, Shanghai, People's Republic of China

\*These authors contributed equally to this work

**Abstract:** Major depression is a complex neuropsychiatric disorder with few treatment approaches. The use of nontargeted antidepressants induced many side effects with their low efficacy. A more precise targeting strategy is to develop nanotechnology-based drug delivery systems; hence, we employed solid lipid nanoparticles (SLNs) to encapsulate HU-211 and curcumin (Cur). The antidepressant effects of the dual-drug nanoparticles (Cur/SLNs-HU-211) for major depression treatment were investigated in corticosterone-induced cellular and animal models of major depression. Cur/SLNs-HU-211 can effectively protect PC12 cells from corticosterone-induced apoptosis and can release more dopamine, which may be associated with the higher uptake of Cur/SLNs-HU-211 shown by cellular uptake behavior analysis. Additionally, Cur/SLNs-HU-211 significantly reduced the immobility time in forced swim test, enhanced fall latency in rotarod test, and improved the level of dopamine in mice blood. Cur/SLNs-HU-211 can deliver more Cur to the brain and thus produce a significant increase in neurotransmitters level in brain tissue, especially in the hippocampus and striatum. The results of Western blot and immunofluorescence revealed that Cur/SLNs-HU-211 can significantly enhance the expression of CB1, p-MEK1, and p-ERK1/2. Our study suggests that Cur/SLNs-HU-211 may have great potential for major depression treatment.

**Keywords:** major depression, curcumin, HU-211, solid lipid nanoparticles, dopamine

## Introduction

Major depression, one of the most prevalent forms of mental illnesses, is known to be the fourth most prevalent disease now, and by 2020 is expected to be the second most prevalent. With an increasing morbidity worldwide, it induced serious personal suffering and economic loss.<sup>1,2</sup> Major depression has long been deemed as a physiological adaptation to pathologic change in brain,<sup>3</sup> and the brain is probably one of the least accessible organs, owing to the existence of the blood-brain barrier (BBB), which prevents the entry of antidepressant drug molecules into brain.<sup>4</sup> Thus, overcoming the BBB is indispensable for successful treatment of major depression. In addition, the antidepressants have significant adverse effects including sexual dysfunction, cardiotoxicity, and sleeping trouble.<sup>5</sup> Therefore, new therapeutic approaches for major depression treatment are desirable.

Corticosterone (CORT), a kind of glucocorticoid, is closely associated with depression. Administration of CORT was usually used for the establishment of major depression model in vitro and in vivo. It has been reported that CORT can induce

Correspondence: Shilong Wang;  
Rongrong Zhu  
Research Center for Translational Medicine at East Hospital, School of Life Science and Technology, Tongji University, 1239 Siping Road, Shanghai 200092, People's Republic of China  
Tel +86 21 6598 2595  
Fax +86 21 6598 2286  
Email wsl@tongji.edu.cn; rrzhu@tongji.edu.cn

the apoptosis and damage of PC12 cells, depression-like behavior, neurochemistry, and brain anatomy changes in animal.<sup>6–10</sup> Additionally, we have enough reasons to believe that the drug that can reverse CORT-induced neurotoxicity may have a possible therapeutic potential in preventing or treating major depression.

Curcumin (Cur), an orange-yellow powder, is the main biologically active principle of turmeric (*Curcuma longa*). Cur exhibits various pharmacological activities including antioxidant activities, immunomodulatory activities, and neuroprotective activities.<sup>11–13</sup> More recently, it has been found that Cur has antidepressant effects on major depression model both in vitro and in vivo. Cur seems to display its antidepressant role by protecting the function of monoaminergic systems and controlling the release of neurotransmitters including dopamine (DA), noradrenaline (NE), and 5-hydroxyindoleacetic acid (5-HIAA).<sup>14–16</sup> Nevertheless, the exact mechanism of its antidepressant activity still remains to be explored. Altogether, Cur as a potent approach may show great potential in the management of major depression. Dexanabinol (HU-211) is an artificially synthesized cannabinoid derivative and lacks cannabimimetic effects. HU-211 exhibits not only the antioxidant and neuroprotective activities in brain but also anti-inflammatory activity by inhibiting NF- $\kappa$ B and decreasing cytokines such as TNF $\alpha$  and interleukin-6, which could ensure the integrity of BBB and reduce cell apoptosis and death. HU-211 is widely used in head injury or stroke treatment and has been shown to be safe in animals and humans.<sup>17–20</sup> With a highly lipophilic nature, HU-211 offers a new treatment approach for major depression.

Although Cur has been deemed as the most credible and promising drug with high efficacy for the treatment of major depression, its drawbacks such as extremely low solubility in water, poor permeability cross the BBB, and poor bioavailability are still the major challenges that make Cur difficult for use as an ideal antidepressant.<sup>21–23</sup> Meanwhile, HU-211 was also hindered by its low stability in biological systems and poor cellular uptake. To circumvent these drawbacks, nanotechnology-based drug delivery systems are promising approaches to improve Cur and HU-211 for better use in major depression treatment. Solid lipid nanoparticles (SLNs) have great potential in delivering drugs to the brain. They display various advantages over other nanoparticles, such as: 1) excellent bioavailability of the carrying agent; 2) controlled drug release; 3) long circulation time in the blood owing to its size; 4) high drug loading; 5) biodegradable and biocompatible properties; and 6) nontoxic nature. As a result, they were accepted by the US

Food and Drug Administration.<sup>24–27</sup> More importantly, SLNs can easily cross the BBB for various reasons; the lipid nature and the small size of SLNs increase the time for them to contact with the BBB further produce a concentration gradient cross the BBB.<sup>28</sup> Additionally, SLNs can easily avoid the P-glycoprotein (P-gp) efflux activity at brain endothelial cells.<sup>29</sup> Polyoxyethylene (40) stearate (Myrj52), a material used for modifying SLNs, can modulate drug uptake via inhibiting the activity of P-gp.<sup>30,31</sup>

In this paper, we aimed to develop and assess SLNs containing Cur and HU-211 (Cur/SLNs-HU-211) for achieving better antidepressant activity. We first synthesized Cur/SLNs-HU-211 via an emulsification and low-temperature solidification method and examined by means of various apparatus, and then the antidepressant activities of nanoparticles in CORT-induced major depression model were investigated in vitro and in vivo.

## Materials and methods

### Materials

Cur and CORT were bought from Aladdin Chemistry Co. Ltd. (Shanghai, People's Republic of China). Polyoxyethylene (40) stearate (Myrj52) was purchased from Sigma Aldrich (St Louis, MO, USA). Stearic acid, chloroform, and lecithin were obtained from Sinopharm Chemical Reagent Co, Ltd. (Shanghai, People's Republic of China). HU-211 was obtained from Cayman Chemical (Ann Arbor, MI, USA). Dulbecco's Modified Eagle's Medium (high glucose), fetal bovine serum, horse serum, penicillin G, streptomycin, and trypsinase were obtained from Gibco (BRL, Grand Island, NY, USA). The other chemical reagents were all analytical grade; water used in all experiments was deionized water.

### Cell culture and animals

Rat pheochromocytoma cells (PC12) were maintained in Dulbecco's Modified Eagle's Medium (high glucose) medium containing penicillin (100 unit/mL), streptomycin (100  $\mu$ g/mL), 5% fetal bovine serum, and 10% horse serum in a 5% CO<sub>2</sub> humid incubator at 37°C.

Female C57BL/6 mice (5–6 weeks old) were purchased from Laboratory Animal Center of Tongji University. Upon arrival, the mice were housed under SPF conditions at 23°C with a 12-hour light–dark cycle, supplied with sufficient food and water. All experiments were in compliance with the Guide for the Care and Use of Laboratory Animals of the National Institutes of Health. The protocol was approved by the Institute of Laboratory Animal Resources of Tongji University. Ethical and legal approval for this study was

obtained from the Institute of Laboratory Animal Resources Animal Care and Use Committee. All efforts were made to minimize animal suffering and sacrifice.

## Preparation of nanoparticles

Cur/SLNs-HU-211 was developed by using an emulsification and low-temperature solidification method. The lipophilic material was dissolved in a water-immiscible organic solvent that was emulsified in an aqueous phase. Upon evaporation of the solvent, a nanoparticle dispersion was formed by precipitation of the lipid in the aqueous medium. In brief, a total of 10 mL solution containing Cur (0.15 g), stearic acid (0.2 g), lecithin (0.1 g), and HU-211 (0.002 g) were prepared in chloroform and then added into 30 mL of H<sub>2</sub>O containing Myrj52 (0.25 g) under fast stirring; the mixture was stirred at 1,200 rpm at 75°C for about 1 hour till the total volume reduced to 5 mL, and then 10 mL of cold water was added and the solution was stirred at 1,200 rpm for another 2 hours at 0°C and centrifuged at 20,000 rpm (Avanti J25 centrifuge, JA25.50 rotor, Beckman) to collect the synthesized materials. The productive Cur/SLNs-HU-211 was dried for 24 hours at -56°C in vacuum. The blank SLNs were developed following the same procedure without the addition of Cur and HU-211, and the preparation of Cur/SLNs was done using the same protocol without the use of HU-211.

## Characterization of nanoparticles

The morphology and structure of Cur/SLNs-HU-211 nanoparticles were observed by means of transmission electron microscopy (JEOL, Tokyo, Japan). In short, a drop of solution (2 mg/mL) was put on the copper grids and negatively stained with (1%, w/v) sodium phosphotungstate. Zeta potential was measured using a Malvern zetasizer Nano ZS (Malvern Instrument, UK). The chemical interactions between Cur, HU-211, and SLNs were confirmed by Fourier transform infrared spectroscopy (FTIR) using a Nicolet 6700 FTIR spectrometer (Bruker Vector 22, USA) in the range of 500–4,000/cm. The crystallographic structures of the SLNs, Cur, Cur/SLNs, and Cur/SLNs-HU-211 were characterized using an X-ray diffractometer (D8 Advance; Bruker Corporation) in the range of 10°–70°, at a voltage of 40 kV and a current of 40 Ma.

The content of loaded Cur was determined by ultraviolet–visible (UV–vis) spectroscopy; a certain amount of Cur/SLNs and Cur/SLNs-HU-211 nanoparticles were dissolved in ethanol and measured at 425 nm. The concentration of Cur was calculated according to a standard curve. The amount of entrapped HU-211 was determined by high-pressure

liquid chromatography (HPLC, Agilent 1100) with C18 column (25 cm × 4.6 mm, 5 μm). The mobile phase used was of a mixture of methanol/water (70/30, v/v), at a flow rate of 0.5 mL/minute, and the detection was performed at 270 nm. Samples (20 μL) were injected manually.

## Solubility and in vitro release

Cur, Cur/SLNs, and Cur/SLNs-HU-211 at equal Cur dose were dissolved in phosphate-buffered saline (PBS; 0.01 M, pH 7.4) to compare their aqueous solubility. Furthermore, the Cur release from Cur/SLNs-HU-211 was investigated using a dialysis membrane in PBS (pH 7.4). Briefly, 2 mL of Cur/SLNs-HU-211 solution (10 mg/mL) was introduced into a dialysis bag (cutoff size 14 kDa). The bag was then put into 500 mL PBS (pH 7.4) containing 10% Tween 80 (v/v) and stirred at 100 rpm at 37°C. At predetermined time points, 4 mL solution was taken out to detect the concentration of Cur by UV–vis spectroscopy, and then the same volume of fresh media was added to maintain constant volume.

## CORT-induced major depression model in PC12 cells and effect of Cur on major depression model in vitro

First, an appropriate major depression model in PC12 cells was investigated. Then, various concentrations of CORT (100, 200, 300, 400, 500, 600, and 700 μM) were incubated with PC12 cells for 24 hours, and cell viability was determined by MTT assay. An appropriate concentration of CORT was used in subsequent in vitro experiments.

To research the effect of Cur on major depression model, the cells were divided into five groups: nontreated control, CORT, and CORT plus Cur (0.04, 0.2, and 1 μM). Analysis was performed 24 hours after the cells were seeded. Cur was applied 2 hours prior to CORT treatment; the cells were cultured for another 24 hours. Viability was then determined by the MTT assay.

## MTT assay

To study the protective effect of Cur/SLNs-HU-211, the cells were seeded in a 96-well plate and divided into seven equal groups: CORT plus PBS, nontreated control, CORT plus Fluoxetine (1 μM), HU-211, Cur, Cur/SLNs, and Cur/SLNs-HU-211 at a Cur concentration of 0.2 μM. Treatments were performed 24 hours after the cells were seeded. All groups were treated for 2 hours prior to the addition of CORT, and then the cells were coincubated for another 24 hours. Cell viability was obtained by the MTT assay.<sup>32</sup> At the end of

treatment, the medium was replaced with 0.5 mg/mL MTT and cultured for another 4 hours at 37°C. Then, dimethyl sulfoxide (DMSO) was added to dissolve formazan crystals. After shaking for 10 minutes at room temperature, the absorbance at 492 nm was measured using a microplate reader (ELX 800 UV, BIO-TEK, USA). The results of cell viability were presented as a percentage of nontreated control.

## DA release detection

To study the protective effect of Cur/SLNs-HU-211, DA release from PC12 cells was detected. The cells were seeded in a 12-well plate, and the division of groups was same as used for MTT assay. After treating for another 24 hours, the culture medium was collected. To determine the DA concentration in the medium for different treatments, an HPLC method was used. Separation was carried out with a mobile phase consisting of methanol/0.01 M  $\text{KH}_2\text{PO}_4$  (10:90, v/v, pH 3.5) at a flow rate of 0.5 mL/minute and a detection wavelength of 280 nm. Standard DA sample was also detected using the same procedure; concentration of DA in the medium was calculated according to a standard curve.

## Cellular uptake observation

To analyze the cellular uptake behavior of Cur, Cur/SLNs, and Cur/SLNs-HU-211, PC12 cells were seeded in a 12-well plate and grown for 24 hours. Then, the medium was changed with fresh solution containing test materials (CORT plus Cur, Cur/SLNs, and Cur/SLNs-HU-211 at a Cur concentration of 1  $\mu\text{M}$ ); the cells were treated for 1, 2, 4, and 8 hours, respectively. After that, the cells were washed three times with PBS, collected, and washed twice for detection with a flow cytometry (Becon, Dickinson and Company, Mountain View, CA, USA).

## Western blot analysis

The group division was the same as that used for the MTT assay, only the Cur dose was increased to 1  $\mu\text{M}$ . At the end of different treatments (after 24 hours), PC12 cells were harvested and washed once with PBS. A total protein extraction kit (KenGen, Biotech, Co. Ltd.) was used to purify protein. The whole cell lysates were centrifuged at 13,000 rpm for 20 minutes at 4°C to collect the supernatants. The concentration of protein was determined by bicinchoninic acid protein assay (KenGen, Biotech, Co. Ltd.). Equal amounts of proteins were separated with an sodium dodecyl sulfate (SDS) polyacrylamide gel and transferred to a polyvinylidene difluoride (PVDF) membrane. Then, the membrane was blocked with 5% (w/v) bovine serum albumin (BSA) in Tris Buffered

Saline with Tween 20 (TBST) for 1.5 hours and incubated overnight at 4°C with the primary antibodies (CB1, p-MEK1, and p-ERK1/2) following manufacturer's instructions. After washing three times with TBST, the membrane was incubated with second antibody for 1 hour at room temperature. After washing three times with TBST, the bands were observed using a chemiluminescence detection system (Santa Cruz Biotechnology, Santa Cruz, CA, USA).

## CORT-induced major depression mice model

The major depression mouse model was established by repeated administration of CORT. Mice were injected with CORT (40 mg/kg) every morning for 21 days (according to a previously published protocol).<sup>33</sup> Mice untreated with CORT were set as normal control group. Forced swim test (FST) and rotarod test were used to examine the success of CORT-induced depression-like behavior changes; mice those who failed the tests were abandoned.

Once the major depression model was established, all mice, including normal mice, were randomly assigned to seven groups: Group I, mice with major depression that received PBS; Group II, seven normal control mice; Group III, mice with major depression that were treated with fluoxetine; Group IV, mice with major depression that were subjected to HU-211; Group V, mice with major depression that received Cur; Group VI, mice with major depression that were treated with Cur/SLNs; and Group VII, mice with major depression that were injected with Cur/SLNs-HU-211. Cur (20 mg/kg), freshly dissolved in normal saline, was administered by intraperitoneal injection every day for 2 weeks. Fluoxetine (40 mg/kg) was used as a positive control drug. Groups VI and VII were given equal Cur dose in Group V according to drug loading, respectively. For group IV, mice subjected to HU-211 were treated according to drug loading of Cur/SLNs-HU-211.

## Behavioral change observation

FST was applied to assess the effect of Cur/SLNs-HU-211 on mice with major depression. A modified procedure was performed following a previously published method.<sup>34</sup> Mice were introduced into glass cylinders (height 25 cm, diameter 10 cm, water 6 cm at 23°C) for 8 minutes individually. A video camera was used for recording the activity of mice. Since the mice were mostly mobile for the first 2 minutes, the last 6 minutes were counted by a scorer that was blinded to the experiment. A mouse was considered immobile only when it stopped struggling, remained floating in the water,

and made necessary moves only to maintain balance. The water was changed between each session.

After the drug was given, a rotarod apparatus with automatic falling sensors and timers was used to evaluate motor performance in different groups.<sup>35</sup> The performance was determined via measuring the latency of mice to stay on a 3 cm diameter drum accelerated from 4 to 40 rpm. The latency to falling was recorded automatically. To get a baseline, pretraining was conducted three times per day for 3 days before the rotarod test. The data were analyzed by a scorer blinded to the group design.

### Serum DA level

Blood samples were collected from mice before they were sacrificed, kept in clean tubes, and centrifuged to get serum. About 100  $\mu$ L of serum was mixed with equal volume of acetonitrile to precipitate DA, and centrifuged at 10,000 rpm for 15 minutes to obtain the supernatant. Immediately, the supernatant was analyzed using the HPLC method as described earlier.

### Body weight

Mice were weighted before being injected with drug throughout the whole experiment and the experiments were never performed after food or water deprivation.

### Tissue sampling

The mice were sacrificed at the end of the experiment; tissue samples (kidney, liver, lung, heart, and brain) were taken out 0.5 hour after the last drug treatments. Meanwhile, the brain samples including hippocampus, brainstem, cortex, striatum, and cerebellum were collected in duplicate: one for the detection of neurotransmitters, and the other for immunofluorescence analysis. The samples were stored at  $-80^{\circ}\text{C}$  until used for further biochemical estimations.

### In vivo distribution of Cur

Tissue samples were homogenized to analyze the distribution of Cur in kidney, liver, lung, heart, and brain. For a 200  $\mu$ L sample, 200  $\mu$ L of acetonitrile was added and the mixture was centrifuged at 10,000 rpm for 15 minutes. The supernatant was then determined by HPLC to detect Cur using a modified method. Separation was carried out with a mobile phase consisting of methanol and 0.5%  $\text{CH}_3\text{COOH}$  (44:56) at a flow rate of 0.5 mL/minute with a 420 nm detection wavelength. Standard Cur sample was also detected using the procedure, and concentration of Cur in tissue was calculated according to a standard curve. Meanwhile, a bicinchoninic acid protein

assay kit was used to quantify the protein concentration of tissue immediately after homogenization.

### Brain neurotransmitters analysis

Hippocampus, brainstem, cortex, striatum, and cerebellum were separated from brain and homogenized; then, an equal volume of acetonitrile was added and the mixture centrifuged to get supernatant. The supernatant was then determined by HPLC. Concentration of DA was determined according to the method described in the "Serum DA level" section. In addition, NE and 5-HIAA were also measured via HPLC. For NE, the mobile phase consisted of methanol/0.05 M  $\text{CH}_3\text{COONa}$  (60:40, v/v), at a flow rate of 0.5 mL/minute and a detection wavelength of 275 nm. For 5-HIAA, the mobile phase consisted of methanol/0.05 M  $\text{KH}_2\text{PO}_4$  (8:92, v/v, pH 4.0), at a flow rate of 0.5 mL/minute and a detection wavelength of 275 nm. Standard sample was also used. A bicinchoninic acid protein assay kit was used to quantify the protein concentration of brain immediately after samples were homogenized.

### Immunofluorescence

To observe the effect of the treatments on brain histology, the mice brain tissues (including hippocampus, brainstem, cortex, striatum, and cerebellum) were kept in 4% paraformaldehyde for fixing, then imbedded in paraffin wax, and sliced into 40  $\mu$ m sections using a vibratome (Leica). A super fluorescein isothiocyanate immunofluorescence detection system kit (Bioworld, MN, USA) was used for incubation with primary antibody (CB1, p-MEK1, and p-ERK1/2) according to the manufacturer's recommended protocol. Finally, the samples were observed under a fluorescence microscope.

### Statistical analysis

The results are presented as the mean  $\pm$  standard deviation (SD). Statistical analysis was performed using the Statistical Product and Service Solutions software. One-way analysis of variance was used for every statistical analysis. Statistical significance was set at *P*-value less than 0.05.

## Results

### Characterization of nanoparticles

Cur/SLNs-HU-211 was successfully prepared such that it achieved the ability to cross BBB.<sup>30,31</sup> The nanoparticles were characterized by various methods. As can be seen from the transmission electron microscopic images (Figure 1A), Cur/SLNs-HU-211 had a spherical shape and uniform size. Zeta potential distribution (Figure 1B) revealed that SLNs

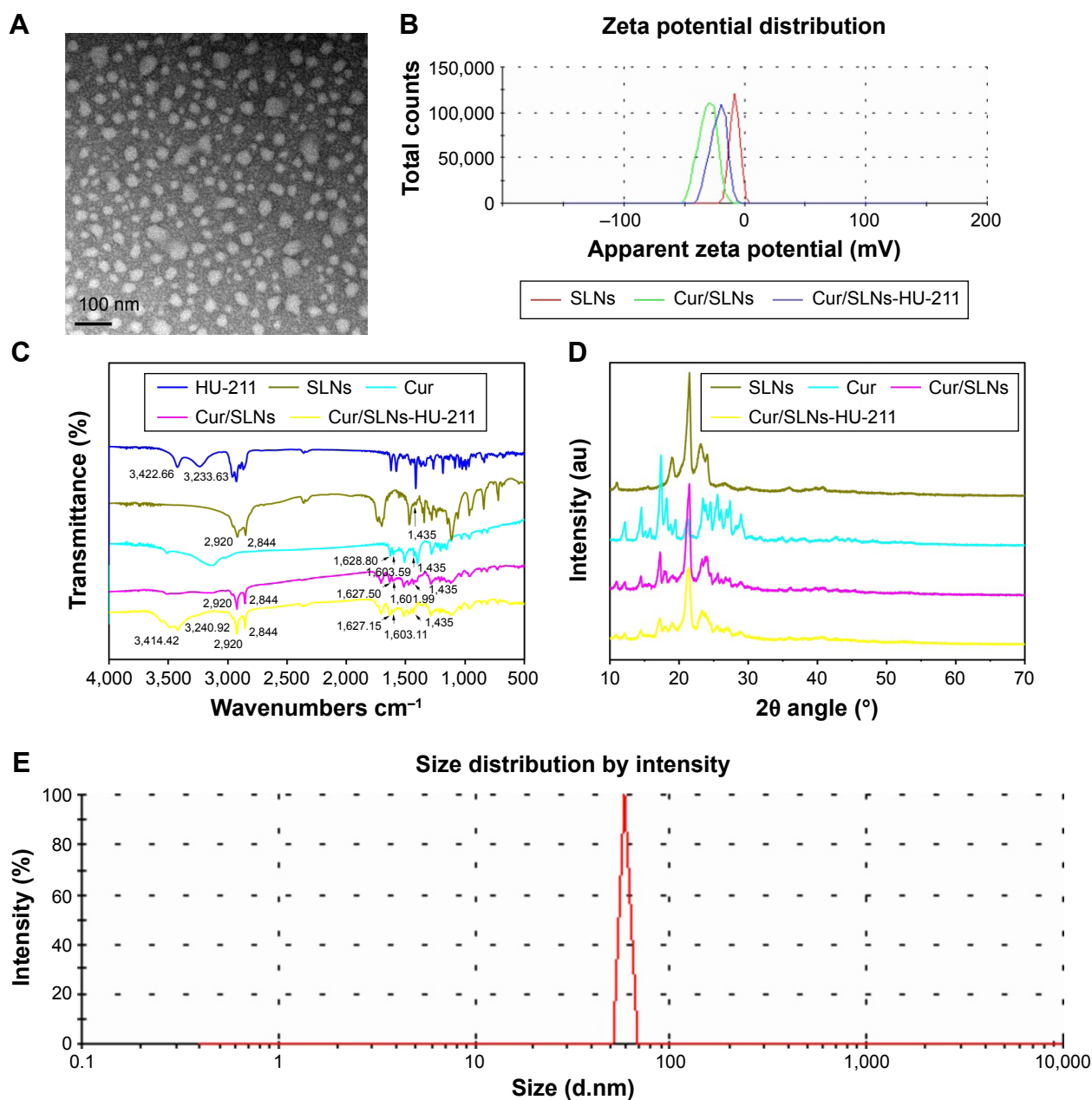


**Figure 1** Transmission electron microscopy images of Cur/SLN-HU-211 (A); zeta potential measurements for HU-211, SLNs, Cur, Cur/SLN, and Cur/SLN-HU-211 (B); Fourier transform infrared spectra (C); X-ray powder diffraction pattern of SLNs, Cur, Cur/SLN, and Cur/SLN-HU-211 (D); and dynamic light scattering study of Cur/SLN-HU-211 (E).

**Abbreviations:** Cur/SLN-HU-211, curcumin and HU-211 coencapsulated solid lipid nanoparticles; HU-211, dexanabinol; SLNs, solid lipid nanoparticles; Cur/SLN, Cur-loaded SLNs; Cur, curcumin.

( $-8.4 \pm 0.6$  mV), Cur/SLN ( $-32.1 \pm 1.3$  mV), and Cur/SLN-HU-211 ( $-21.7 \pm 0.4$  mV) exhibited negative zeta potential. As shown by FTIR spectrum (Figure 1C), two peaks of HU-211 were observed at 3,422.66 and 3,233.63/cm, while SLNs exhibited characteristic peaks at 2,920 and 2,844/cm for the stretching vibration of carboxylic O-H; Cur showed peaks at 1,628.80/cm (C=C) and 1,603.59/cm (aromatic C=C). The peaks at 1,435/cm in both SLNs and Cur may due to the deformation and stretching of methyl groups ( $-\text{CH}_3$ ).

The spectrum of Cur/SLN showed that Cur was well encapsulated by SLNs, as all of the characteristic peaks of Cur were found, and the spectrum of Cur/SLN-HU-211 implied that HU-211 and Cur were all encapsulated by SLNs, because all characteristic peaks of HU-211 and Cur were also identified in Cur/SLN-HU-211. The purpose of carrying X-ray powder diffraction was to study the diffraction pattern of Cur/SLN-HU-211 (Figure 1D). Cur showed sharp peaks between  $10^\circ$  and  $30^\circ$ , indicating that Cur was in

a highly crystalline state. This phenomenon did not appear in Cur/SLNs or Cur/SLNs-HU-211, which suggested that the disordered crystalline state Cur was entrapped by the core of SLNs. In addition, the spectrum of Cur/SLNs and Cur/SLNs-HU-211 showed both peaks of SLNs and Cur, only weaker and broader, which implied that Cur was well entrapped by SLNs. Furthermore, Cur/SLNs-HU-211 had weaker and broader peaks as compared to Cur/SLNs – this could largely be due to the addition of HU-211. The disordered-crystalline state of Cur in nanoparticles do help Cur to release from the nanoparticles,<sup>36</sup> thus leading to a sustained release, which is in accordance with our *in vitro* release assay results. Dynamic light scattering study showed that the hydrodynamic size of Cur/SLNs-HU-211 was  $58.77 \pm 1.7$  nm (Figure 1E). The Cur loading of Cur/SLNs and Cur/SLNs-HU-211 was analyzed by UV-vis spectrophotometry and was  $21.61 \pm 1.65\%$  and  $18.34 \pm 1.06\%$ , respectively. The HU-211 loading capacity of Cur/SLNs-HU-211 was determined by HPLC and was  $0.74 \pm 0.02\%$ .

### Solubility and *in vitro* release

We used SLNs to improve the solubility of Cur and to confirm that Cur, Cur/SLNs, and Cur/SLNs-HU-211 in same amount of Cur were suspended in three glass bottles containing 4 mL PBS (pH 7.4) to make a clear comparison (Figure 2A). Cur/SLNs (Figure 2A [b]) and Cur/SLNs-HU-211 (Figure 2A [c]) were well dissolved in PBS; however, Cur (Figure 2A [a]) was still insoluble. To study the potential sustained Cur release from Cur/SLNs-HU-211, 20 mg nanoparticles were put into a dialysis bag. From the release curve (Figure 2B), we observed that there was no remarkable initial burst release during the first 2 days, which meant only a little amount of

Cur was on the surface of the SLNs. Cur/SLNs-HU-211 achieved a sustained release for 7 days, with a total about 77% release; this could be ascribed to the diffusion of Cur in the SLNs.<sup>37</sup>

### Effect of Cur on major depression model in PC12 cells

PC12 cells are usually used for the establishment of major depression model *in vitro*, and this is done by the administration of CORT. To get an appropriate major depression model, PC12 cells were treated with different concentrations of CORT. When treated with 300  $\mu$ M CORT for 24 hours, the cell viability decreased to approximately 50% (Figure 3A), and this value was used in subsequent experiments *in vitro*.

Furthermore, MTT assay was performed to investigate the effect of Cur on CORT-induced apoptosis in PC12 cells. CORT was added 2 hours after Cur treatment. When the cells were cocubated with Cur (0.04, 0.2, and 1  $\mu$ M) for 24 hours, the cell viabilities were about 62.5%, 66.6%, and 69.3% (Figure 3B), indicative of a dose-dependent response. To better study the protective effect of Cur/SLNs-HU-211 on CORT-induced apoptosis in PC12 cells and its possible underlying mechanisms, 0.2  $\mu$ M of Cur was chosen for MTT assay and DA release detection, while 1  $\mu$ M of Cur was selected for Western blot analysis and cellular uptake observation.

### Effect of Cur/SLNs-HU-211 on major depression model in PC12 cells determined by MTT assay and DA release detection

Antidepressants can protect PC12 cells from the apoptosis and neuron damage induced by CORT.<sup>38</sup> MTT assay was

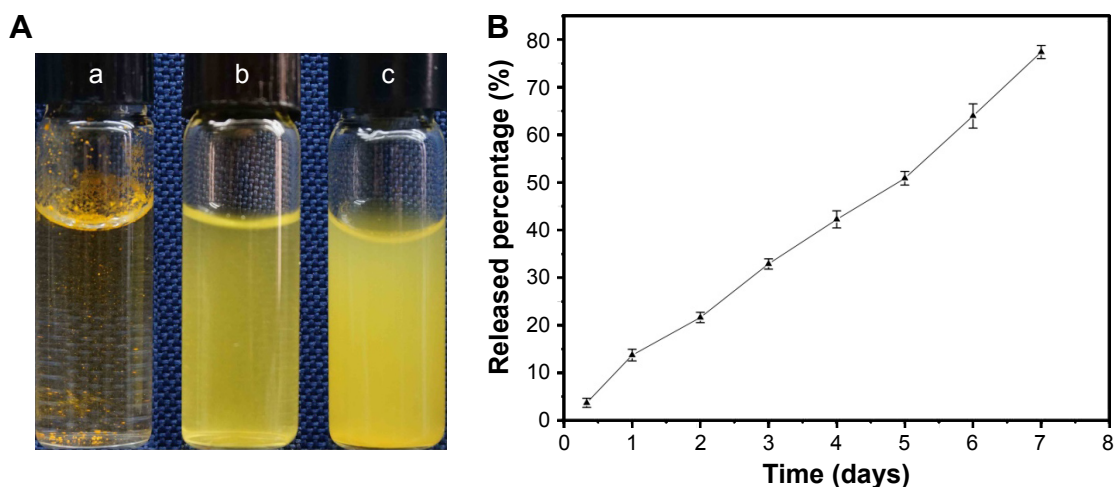


**Figure 2** Solubility study (A) of Cur (a), Cur/SLNs (b), Cur/SLNs-HU-211 (c), and *in vitro* release profiles of Cur in Cur/SLNs-HU-211 (B).

**Abbreviations:** Cur, curcumin; Cur/SLNs, Cur-loaded SLNs; Cur/SLNs-HU-211, curcumin and HU-211 coencapsulated solid lipid nanoparticles.

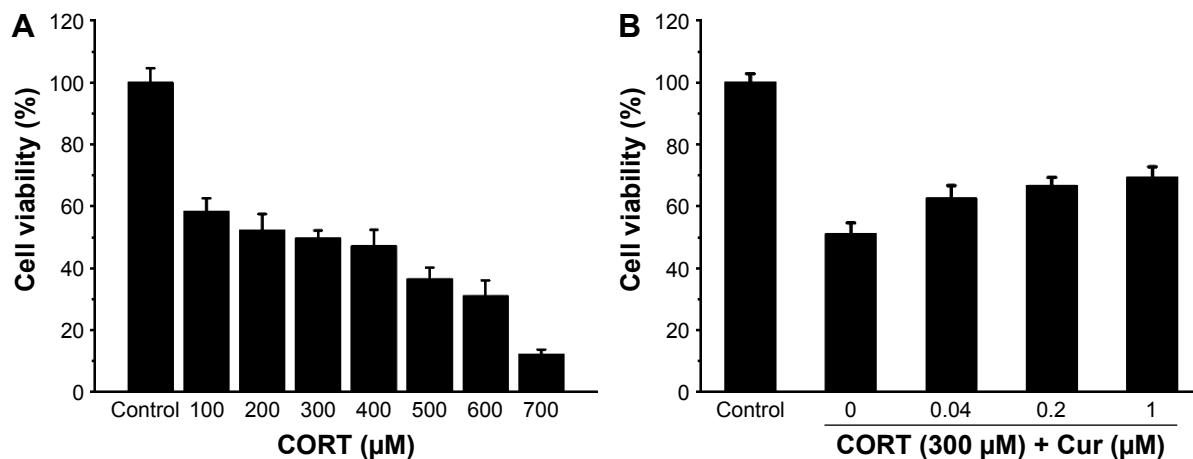


**Figure 3** The effect of CORT on PC12 cell viability determined by MTT assay (A), and the effect of Cur on CORT-induced PC12 cell viability determined by MTT assay (B). **Note:** The results are expressed as mean ± SD. **Abbreviations:** CORT, corticosterone; Cur, curcumin; SD, standard deviation.

performed to evaluate the effect of Cur/SLNs-HU-211 on CORT-induced apoptosis in PC12 cells. Low-dose SLNs were found to be less toxic to cells; thus, it can be considered that the effect of carrier itself is negligible.<sup>39</sup> In MTT assay, after different treatments, PC12 cells' viabilities were measured. Cell viabilities of different groups (PBS, control, Fluoxetine, HU-211, Cur, Cur/SLNs, and Cur/SLNs-HU-211) were 49.4%, 100%, 93.8%, 60.4%, 62.5%, 65.5%, and 73.6%, respectively (Figure 4A). The cell viability of PBS group (treated with CORT only) was significantly lower than others, which further confirmed the successful establishment of the major depression model in PC12 cells.

In addition, Cur/SLNs-HU-211 potentiated its protective effect (increased cell viability) and was significant when compared to HU-211, Cur, and Cur/SLNs, implying that the combination of HU-211 and Cur could achieve enhanced antidepressant activity.

Neurotransmitters including DA, NE, and 5-HIAA play a vital role in the process of depression.<sup>40</sup> DA release detection was employed to investigate the effect of Cur/SLNs-HU-211 on major depression model in PC12 cells. At the end of experiments, cell culture medium was collected and tested by HPLC. DA concentrations for the seven groups (explained in the "CORT-induced major depression mice model" section)

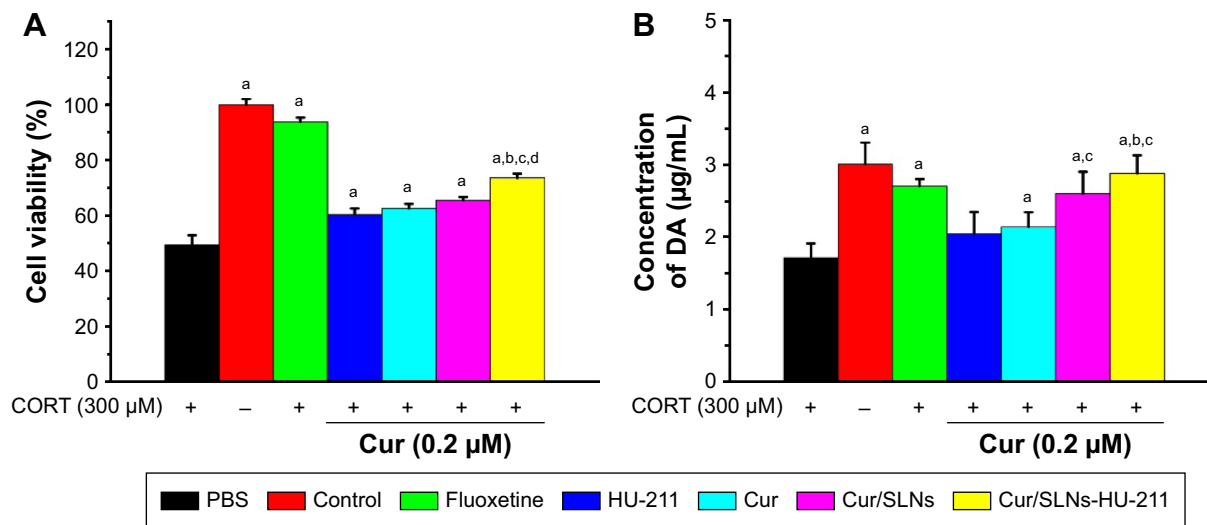


**Figure 4** Protective effect of Cur/SLNs-HU-211 (0.2 μM) against CORT-induced damage in PC12 cells. **Notes:** Cells viability was determined by MTT assay (A) and DA release from PC12 cells (B). The results are expressed as mean ± SD. For statistical significance, <sup>a</sup>P<0.05 as compared to PBS group; <sup>b</sup>P<0.05 as compared to HU-211 group; <sup>c</sup>P<0.05 as compared to Cur group; and <sup>d</sup>P<0.05 as compared to Cur/SLNs group (one-way ANOVA). **Abbreviations:** Cur, curcumin; Cur/SLNs, Cur-loaded SLNs; Cur/SLNs-HU-211, curcumin and HU-211 coencapsulated solid lipid nanoparticles; CORT, corticosterone; DA, dopamine; SD, standard deviation; PBS, phosphate-buffered saline; ANOVA, analysis of variance.



were 1.7, 3.0, 2.7, 2.0, 2.1, 2.6, and 2.8  $\mu\text{g}/\text{mL}$ , respectively (Figure 4B). DA release in PBS group was significantly lower, indicating that the major depression model was successful. Cur/SLNs and Cur/SLNs-HU-21 significantly induced more DA release as compared to PBS. In addition, Cur/SLNs potentiated its protective effect, and this effect was significant compared to Cur. Cur/SLNs-HU-211 induced more DA release as compared to HU-211 and Cur, suggesting that Cur/SLNs-HU-211 use would result in antidepressant activity.

## Cellular uptake observation

For a better Cur detection by flow cytometry, cellular uptake experiment was performed in a higher dose of Cur (1  $\mu\text{M}$ ). Cur was excited at 488 nm for its spontaneous fluorescence. As can be seen from Figure 5, cells treated with Cur/SLNs and Cur/SLNs-HU-211 exhibited much stronger fluorescence as compared to Cur at different time points. About 85% and 99% of the total cells were detected after being treated for 8 hours for Cur/SLNs and Cur/SLNs-HU-211, only 4.15% for Cur, and cellular uptake in PC12 cells was time dependent for each group. Cur/SLNs and Cur/SLNs-HU-211 were easily

taken up by PC12 cells, while Cur could not, which suggested that Cur/SLNs and Cur/SLNs-HU-211 may display stronger protective effect on major depression model than Cur, owing to its enhanced cellular uptake.

## Western blot analysis

MTT assay and DA release detection results revealed that Cur/SLNs-HU-211 had great potential in protecting PC12 cells from CORT-induced damage. To further explore the underlying mechanism, Western blot analysis was performed. Several studies have shown that CB1 cannabinoid receptors are important for major depression – the activation of CB1 is related to activation of downstream signaling molecules such as ERK1/2.<sup>41,42</sup> This occurs via an upstream MEK1 response, but CORT can selectively reduce p-ERK1/2, and the inhibition of ERK1/2 was associated with cell apoptosis.<sup>43,44</sup> Hence, in Western blot, we measured the protein expression level of CB1, p-MEK1, and p-ERK1/2. The expressions of the three proteins were markedly decreased in the CORT-treated group as compared to the normal control, which was also suggestive of a successful major depression model in PC12 cells (Figure 6).

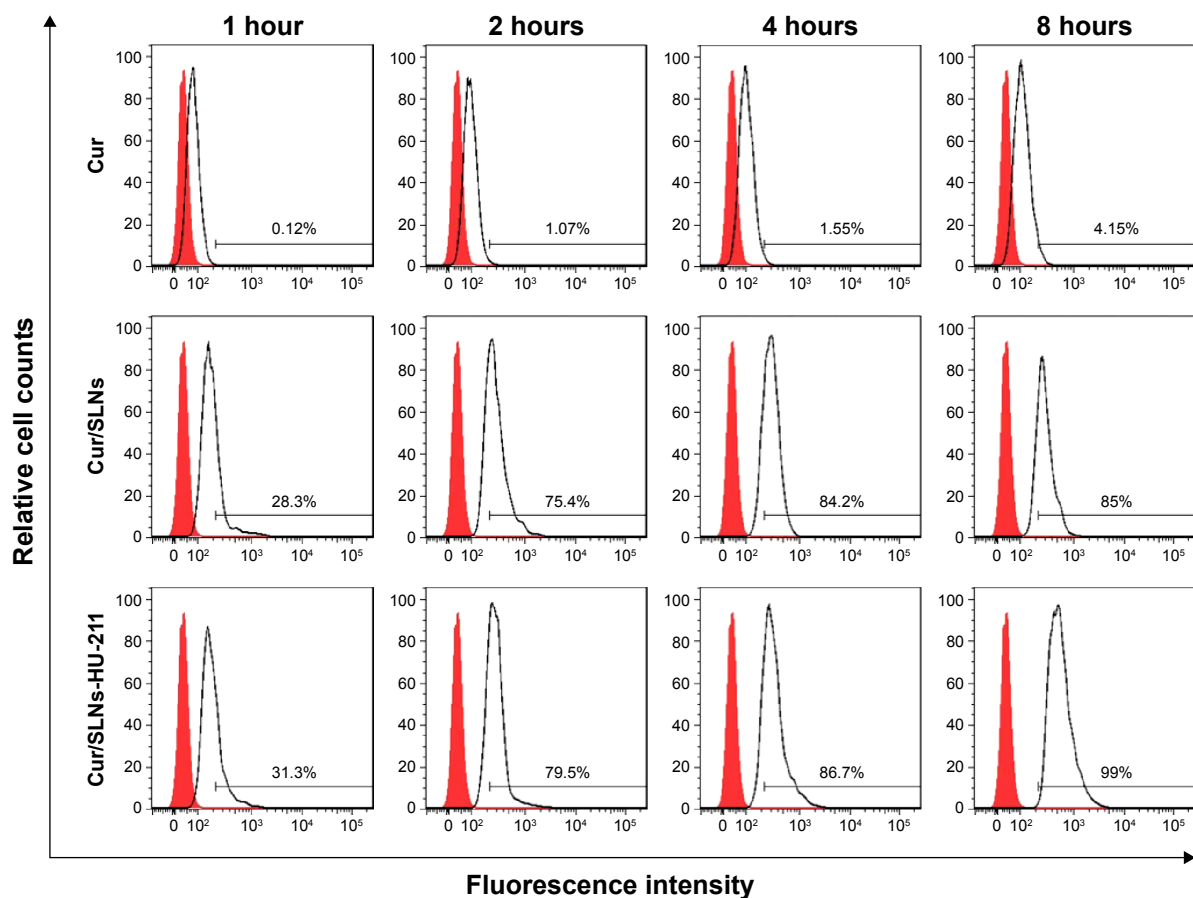


**Figure 5** Cellular uptake observation of Cur/SLNs-HU-211 (1.0  $\mu\text{M}$ ) in PC12 cells by flow cytometry at 1, 2, 4, and 8 hours.

**Abbreviations:** Cur, curcumin; Cur/SLNs, Cur-loaded SLNs; Cur/SLNs-HU-211, curcumin and HU-211 coencapsulated solid lipid nanoparticles.

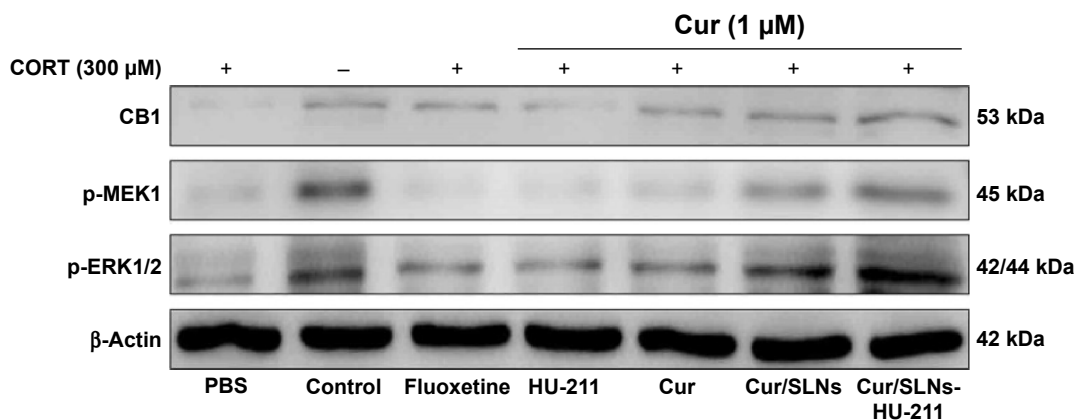


**Figure 6** The effect of Cur/SLN-HU-211 (1.0  $\mu$ M) on the MEK1/ERK1/2 signaling pathway in the CORT-induced major depression model.

**Note:** Representative Western blot images for CB1, p-MEK1, and p-ERK1/2 protein from PC12 cells.

**Abbreviations:** Cur, curcumin; Cur/SLN, Cur-loaded SLNs; Cur/SLN-HU-211, curcumin and HU-211 coencapsulated solid lipid nanoparticles; CORT, corticosterone; PBS, phosphate-buffered saline.

Fluoxetine showed no obvious function, and one possible explanation for this could be that the concentration (1  $\mu$ M) was too low for detection by Western blot. However, the expression of CB1, p-MEK1, and p-ERK1/2 activities were increased in the HU-211 and Cur pretreatment groups; this phenomenon was further enhanced by Cur/SLN and Cur/SLN-HU-211. It is noteworthy that Cur/SLN-HU-211 significantly upregulated the expression of CB1, p-MEK1, and p-ERK1/2 compared with HU-211 and Cur, which suggested that the combination of HU-211 and Cur was advantageous.

### Effect of Cur/SLN-HU-211 on behavioral change and serum DA level

Repeated CORT treatments increase the depression-like behavior. These behavioral changes can be reversed by antidepressants. The FST and rotarod test are reliable and frequently used methods for evaluating the potential of antidepressants. Administration of CORT could also be helpful for the establishment of major depression model in mice. After exposure to CORT for 3 weeks, the mice showed significant increases in the duration of immobility and decreases in fall latency compared with the normal control group. The results of the ethology tests (FST and rotarod test) revealed that the major depression model was successful.

FST and rotarod test were also used to measure the effect of Cur/SLN-HU-211 on major depression model in vivo, and the results of FST (Figure 7A) showed that the mice with major depression showed significant decreases in the duration of immobility when treated with HU-211, Cur/SLN, and Cur/SLN-HU-211 (190, 180, and 160 seconds, respectively) and that Cur/SLN-HU-211 significantly reduced the immobility time as compared to HU-211, Cur, and Cur/SLN. The results of rotarod test (Figure 7B) also revealed

that Cur/SLN (270 seconds) and Cur/SLN-HU-211 (293 seconds) significantly enhanced fall latency in comparison to PBS (247 seconds). Also, Cur/SLN-HU-211 was significantly superior to HU-211, Cur, and Cur/SLN.

Furthermore, we detected the level of DA in mice blood; the results (Figure 7C) demonstrated that Cur/SLN (16.0  $\mu$ g/mL) and Cur/SLN-HU-211 (17.9  $\mu$ g/mL) also induced more DA in blood, and induction of DA by Cur/SLN-HU-211 was obviously higher than that by HU-211, Cur, and Cur/SLN, which was in accordance with the results of FST and rotarod test. In sum, all these ethology tests and biochemical marker measurement suggested that Cur/SLN-HU-211 shows better curative effect in improving the mobility and DA level in vivo.

### Body weight, in vivo distribution of Cur, and measurement of neurotransmitters in brain

Body weight was measured throughout the experiment (Figure 8A), and significant difference was not observed in body weight between the mice in all groups at the end of treatments, indicating the safety of the Cur/SLN and Cur/SLN-HU-211 nanoparticles.

The aforementioned results described inspired us to further investigate the in vivo antidepressant activity of Cur/SLN-HU-211 at the histological level. The biodistribution of Cur was studied by detecting Cur in the groups treated with Cur, Cur/SLN, and Cur/SLN-HU-211 with HPLC. These results (Figure 8B) demonstrate that Cur/SLN-HU-211 enhanced the concentration of Cur in kidney, liver, lung, heart, and brain, and it seems that Cur/SLN-HU-211 accumulated in the brain site for the Cur concentration are significantly higher than the Cur group, this can also

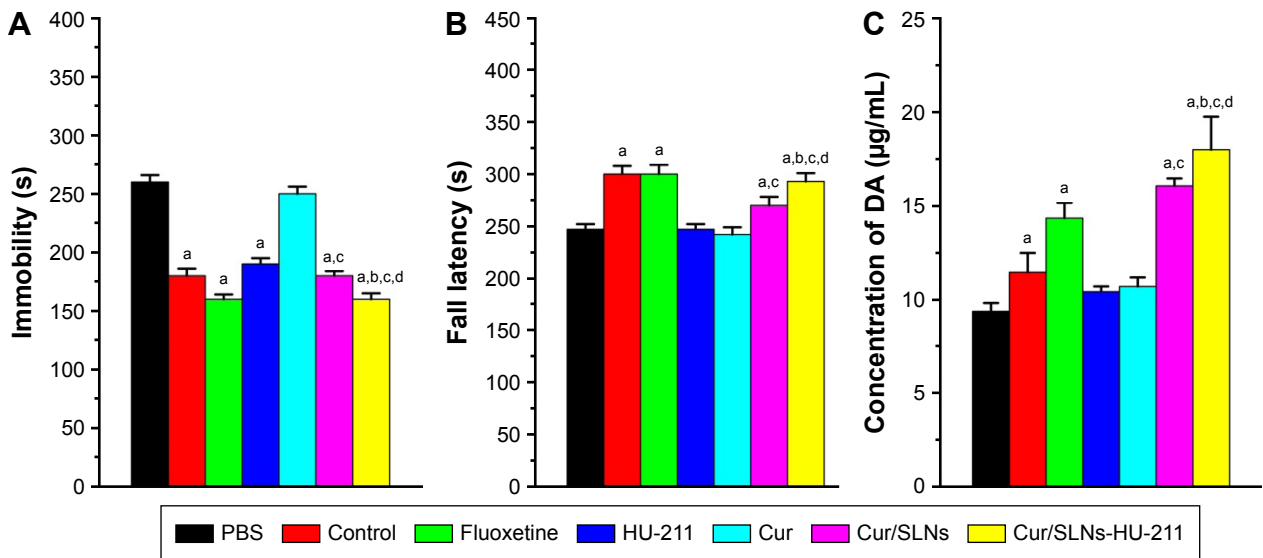


**Figure 7** Effects of Cur/SLNs-HU-211 on the duration of immobility in the forced swim test (A), effects of Cur/SLNs-HU-211 on the fall latency in the rotarod test (B), and effects of Cur/SLNs-HU-211 on serum DA level (C).

**Notes:** The results are expressed as mean ± SD. For statistical significance, <sup>a</sup>*P*<0.05 as compared to PBS group; <sup>b</sup>*P*<0.05 as compared to HU-211 group; <sup>c</sup>*P*<0.05 as compared to Cur group; and <sup>d</sup>*P*<0.05 as compared to Cur/SLNs group (one-way ANOVA).

**Abbreviations:** Cur, curcumin; Cur/SLNs, Cur-loaded SLNs; Cur/SLNs-HU-211, curcumin and HU-211 coencapsulated solid lipid nanoparticles; DA, dopamine; SD, standard deviation; PBS, phosphate-buffered saline; ANOVA, analysis of variance; s, seconds.

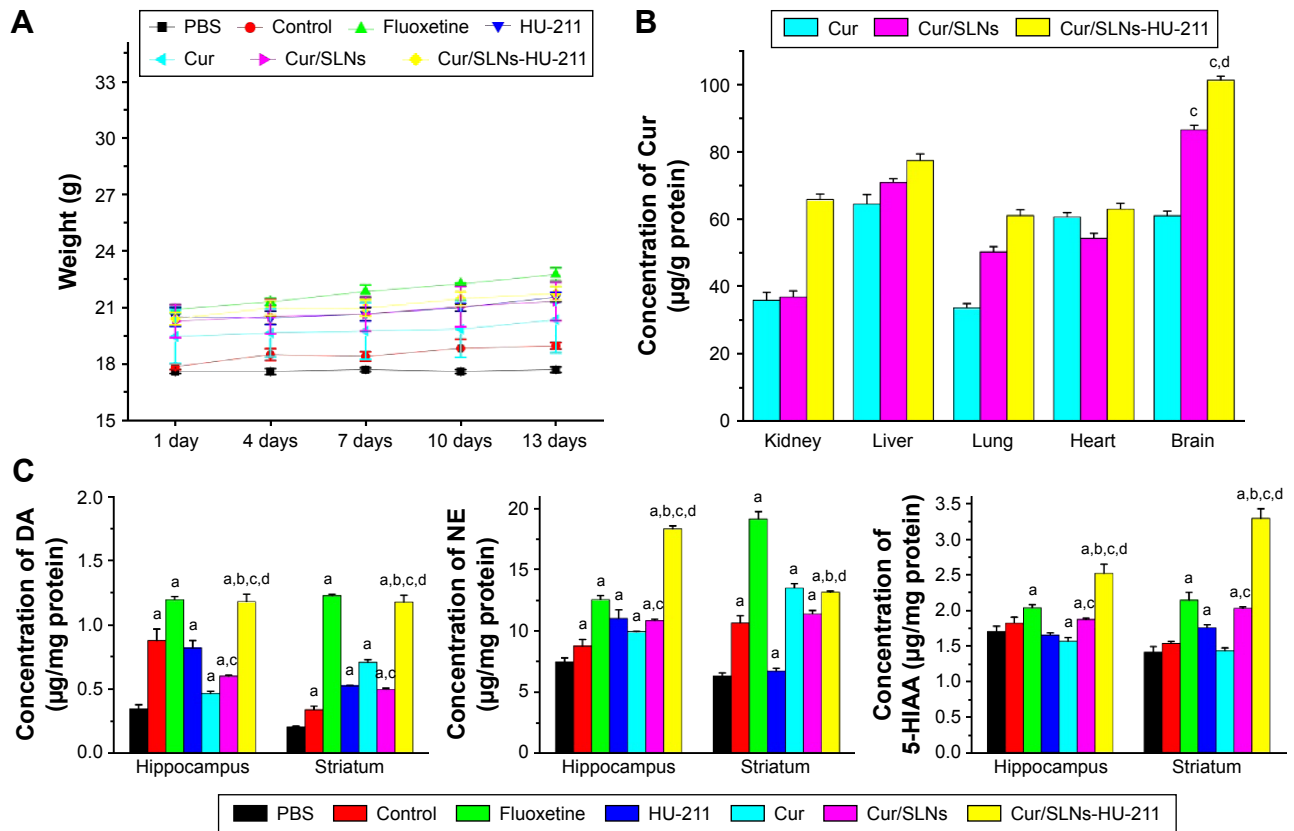


**Figure 8** Body weight change through the whole treatments in each group (A), in vivo Cur distribution after treatment with Cur, Cur/SLNs, and Cur/SLNs-HU-211 (B), and measurement of neurotransmitters in hippocampus and striatum (C).

**Notes:** The results are expressed as mean ± SD. For statistical significance, <sup>a</sup>*P*<0.05 as compared to PBS group; <sup>b</sup>*P*<0.05 as compared to HU-211 group; <sup>c</sup>*P*<0.05 as compared to Cur group; and <sup>d</sup>*P*<0.05 as compared to Cur/SLNs group (one-way ANOVA).

**Abbreviations:** Cur, curcumin; Cur/SLNs, Cur-loaded SLNs; Cur/SLNs-HU-211, curcumin and HU-211 coencapsulated solid lipid nanoparticles; DA, dopamine; NE, noradrenaline; SD, standard deviation; PBS, phosphate-buffered saline; ANOVA, analysis of variance.

be found in Cur/SLNs, which implied that Cur/SLNs and Cur/SLNs-HU-211 can cross the BBB and play their role in the brain. In the presence of HU-211, Cur/SLNs-HU-211 significantly improved the distribution of Cur as compared to Cur/SLNs, proving that HU-211 can improve the ability of SLNs to cross the BBB.

To further research the effect of Cur/SLNs-HU-211 on the brain of mice with major depression, levels of neurotransmitters (DA, NE, and 5-HIAA) were investigated. The content of DA and NE decreased after being treated with CORT in the PBS group compared with the normal control group, which also proved that the major depression model was successfully created (Figure 8C). We also found that Cur/SLNs-HU-211 produced a significant increase in neurotransmitters level in hippocampus and striatum (except NE in striatum) as compared to HU-211, Cur, and Cur/SLNs, suggesting that encapsulating HU-211 and Cur into the same nanoparticle was crucial to exert higher antidepressant activity. No distinct change was observed in brainstem, cortex, and cerebellum, which may be because the Cur/SLNs-HU-211 targets specific brain regions to exert its effects.

## Immunofluorescence

To further demonstrate the results of Western blot in vitro, immunofluorescence of mice brain samples (hippocampus, brainstem, cortex, striatum, and cerebellum) was performed. The results are in accordance with Western blot to a large degree (Figure 9). In the HU-211, Cur, Cur/SLNs, and Cur/SLNs-HU-211 groups, the expressions of CB1, p-MEK1, and p-ERK1/2 proteins were much higher as compared to PBS group (treated with CORT). Among these groups, the Cur/SLNs-HU-211 group showed higher intensity than HU-211, Cur, and Cur/SLNs groups, even higher than normal control or fluoxetine in some cases; this phenomenon was more obvious in hippocampus and striatum. The results of immunofluorescence showed better antidepressant activity of Cur/SLNs-HU-211 on the mice with major depression.

## Discussion

Major depression is a complex mental disorder and the fourth most prevalent disease in the world now. The disease affects about 340 million people worldwide. It has been closely regarded to be related to changes in brain.<sup>3</sup> Although the treatment for major depression has gained considerable progress, the antidepressants now in use still cannot totally meet the needs of the patients, and the molecular mechanism of action of the antidepressants is not fully understood yet. The side effects of classical antidepressants and difficulty of drug molecules in passing through BBB are two major

obstacles for the treatment of depression.<sup>45</sup> New research mostly focus on improving new drugs or formulating brain-targeted delivery systems, and yet only few drugs can cross the BBB and deliver drug in specific brain regions. Thus, developing new safe drugs with high efficacy to achieve precise targeting to the brain is in great urgent.<sup>46</sup>

Cur, a traditional herbal medicine with high efficacy, has many advantages, such as being safe and inexpensive, and is widely used in disorders such as Alzheimer's disease and Parkinson's for its neuroprotective.<sup>47</sup> These days, it has been found that Cur also has the potential as an antidepressant in the treatment of major depression.<sup>48</sup> Few studies concentrated on improving the antidepressant effect of Cur with nanoparticles; the major weakness of Cur includes its low solubility in water and poor bioavailability, which largely limit its application. HU-211 as a low-toxic antidepressant was used in brain diseases; its low stability in biological systems hindered its clinical use.<sup>49</sup> Our previous studies demonstrated that Cur/SLNs showed great potential in anti-inflammatory activity;<sup>39,50</sup> however, its potential to cross BBB and treat major depression is still unknown. In this study, we introduced a highly lipophilic drug HU-211 associated with Cur/SLNs to form a new dual-drug nanoparticle (Cur/SLNs-HU-211) with the hope of enhancing the ability of Cur/SLNs to cross BBB and precisely target the disease lesions.

Cur/SLNs-HU-211 was developed using an emulsification and low-temperature solidification method. In this dual-drug delivery system, SLNs itself can cross the BBB and deliver the drug molecular to a specific brain site; Myrj52 and HU-211 can be used to modify SLNs and enhance this ability, mainly because Myrj52 can inhibit the function of P-gp and because HU-211 is highly lipophilic.<sup>51-53</sup> To confirm the successful fabrication of Cur/SLNs-HU-211, many physicochemical characterizations were performed. Transmission electron microscopy results showed that Cur/SLNs-HU-211 was uniform, which may contribute to better solubility in water and bioavailability in biological system. Its small size prolongs the circulation time in blood and thus increases the opportunity for SLNs to contact with the BBB and produce a concentration gradient across the BBB.<sup>28</sup> A negative potential of  $-21.7$  mV is high enough to avoid the aggregation of nanoparticles and enhance stability.<sup>37</sup> The results of FTIR and X-ray powder diffraction showed that Cur and HU-211 were well encapsulated by SLNs, and the solubility of Cur was also improved by SLNs. The sustained Cur release in Cur/SLNs-HU-211 prolongs its circulation time in the body. All these data suggested the successful design of Cur/SLNs-HU-211.

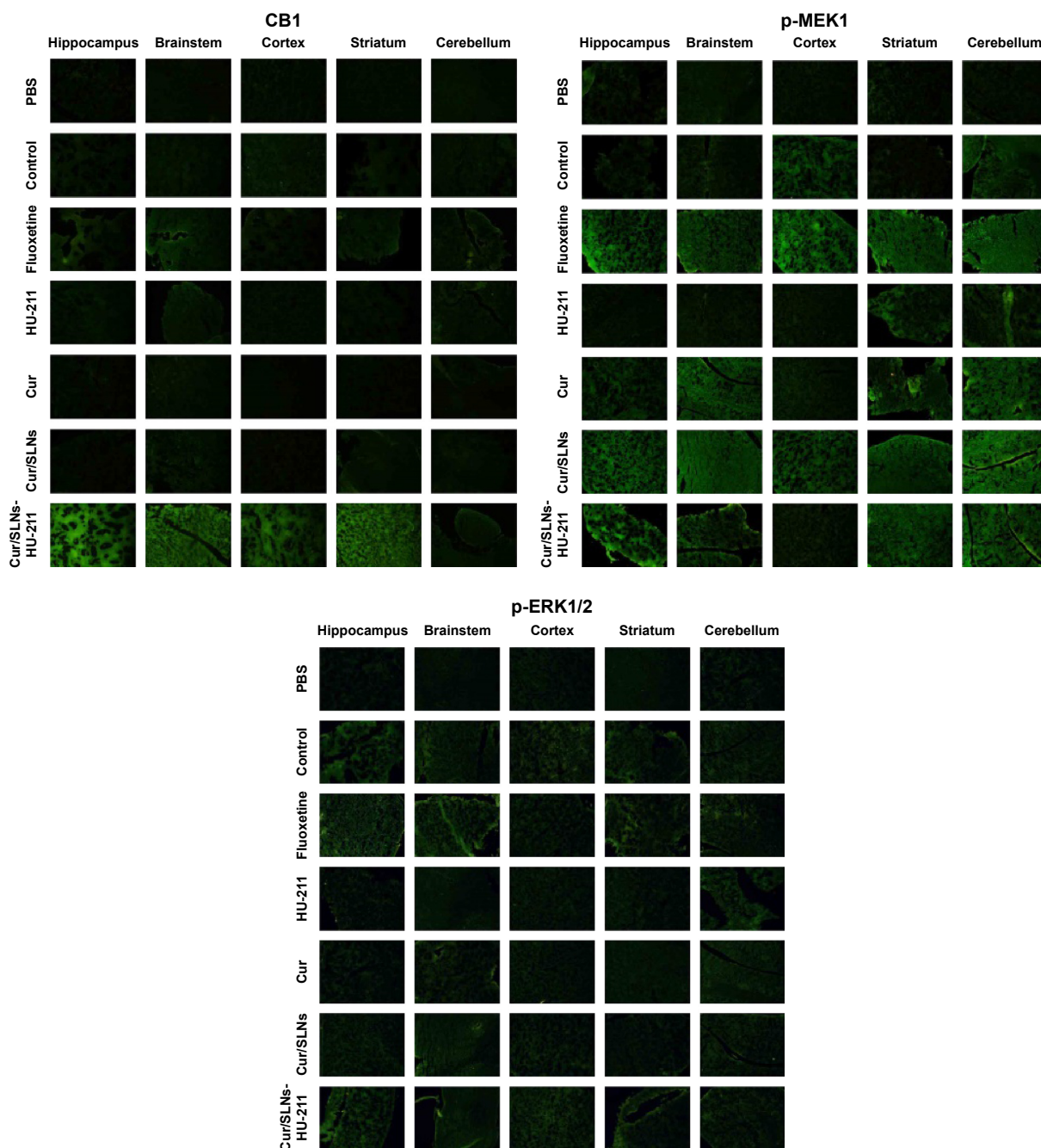


**Figure 9** Representative immunofluorescence images for CB1, p-MEK1, and p-ERK1/2 in different mice brain regions after treatment.

**Abbreviations:** PBS, phosphate-buffered saline; Cur, curcumin; Cur/SLNs, Cur-loaded SLNs; Cur/SLNs-HU-211, curcumin and HU-211 coencapsulated solid lipid nanoparticles.

Then, we investigated the antidepressant activity of Cur/SLNs-HU-211 by using a major depression model *in vitro* and *in vivo*. The major depression model was established by administration of CORT. *In vitro*, cocubation of CORT with PC12 cells causes the apoptosis and damage in PC12 cells, which provides an ideal model system for depression study. *In vivo*, CORT can exert toxic effect on neurons and synapses, further inducing behavioral changes related to depression symptoms.<sup>6,10</sup> To our knowledge, many studies have investigated the effect of antidepressant drug either

*in vitro* or *in vivo*; however, very few have investigated them at the same time.<sup>54,55</sup> In this paper, both *in vitro* and *in vivo* experiments (in PC12 cells and C57BL/6 mice, respectively) were performed.

Cur can activate the MEK1/ERK1/2 signaling pathways through CB1 cannabinoid receptor and modulate the level of neurotransmitters including DA, NE, and 5-HIAA.<sup>15,41,42,56–58</sup> ERK1/2, a member of mitogen-activated protein kinases family, is widely distributed in the mammalian nervous system. It has been reported that ERK1/2 is critical for the functions

of normal brain, cell survival, and major depression. ERK1/2 activation was a receptor-mediated event and occurred via an upstream MEK1 response; the CB1 is linked to MEK1/ERK1/2 signaling, an important pathway to transport the signal from the cell surface to the nucleus. Previous studies have demonstrated that acute tetrahydrocannabinol administration can increase CB1 receptor-mediated ERK1/2 activation in the dorsal striatum and hippocampus.<sup>43,44,59,60</sup> ERK1/2 activation was indispensable for DA release.<sup>61,62</sup> It is well known that neurotransmitters are important in the pathogenesis of depression; they promote neuronal growth and survival. According to a popularly accepted monoamine-deficiency theory, the underlying mechanism of major depression is a lack of neurotransmitters.<sup>63</sup> Antidepressant drugs are supposed to cure major depression effectively by enhancing the availability and level of neurotransmitters.

The main finding of this research is that, in our major depression model in PC12 cells and mice, Cur/SLNs-HU-211 showed impressive protective effect against CORT-induced damage. Cur/SLNs-HU-211 significantly improved the

distribution of Cur in brain and the uptake efficiency in PC12 cells. The expression levels of CB1, p-MEK1, and p-ERK1/2 were upregulated; furthermore, the cell viability and the DA level in medium and serum were significantly improved by Cur/SLNs-HU-211. The levels of neurotransmitters in hippocampus and striatum were significantly higher when treated with Cur/SLNs-HU-211 as compared to PBS (group treated with CORT only); Cur/SLNs-HU-211 also reduced the immobility time in FST and enhanced the fall latency in rotarod test.

On the basis of these results, we infer that Cur/SLNs-HU-211 can readily cross the BBB, thus acting in specific brain region (hippocampus and striatum) and activating the MEK1/ERK1/2 signaling pathway and protecting the cell from CORT-induced damage, thus evoking behavioral change in mice (Figure 10). In our future research, a BBB model and inhibitors associated with the signaling pathways will be applied to further study the underlying mechanism of its activity.<sup>23,64</sup> It is noteworthy that, in this study, the low-toxic Cur/SLNs-HU-211 nanoparticles displayed excellent

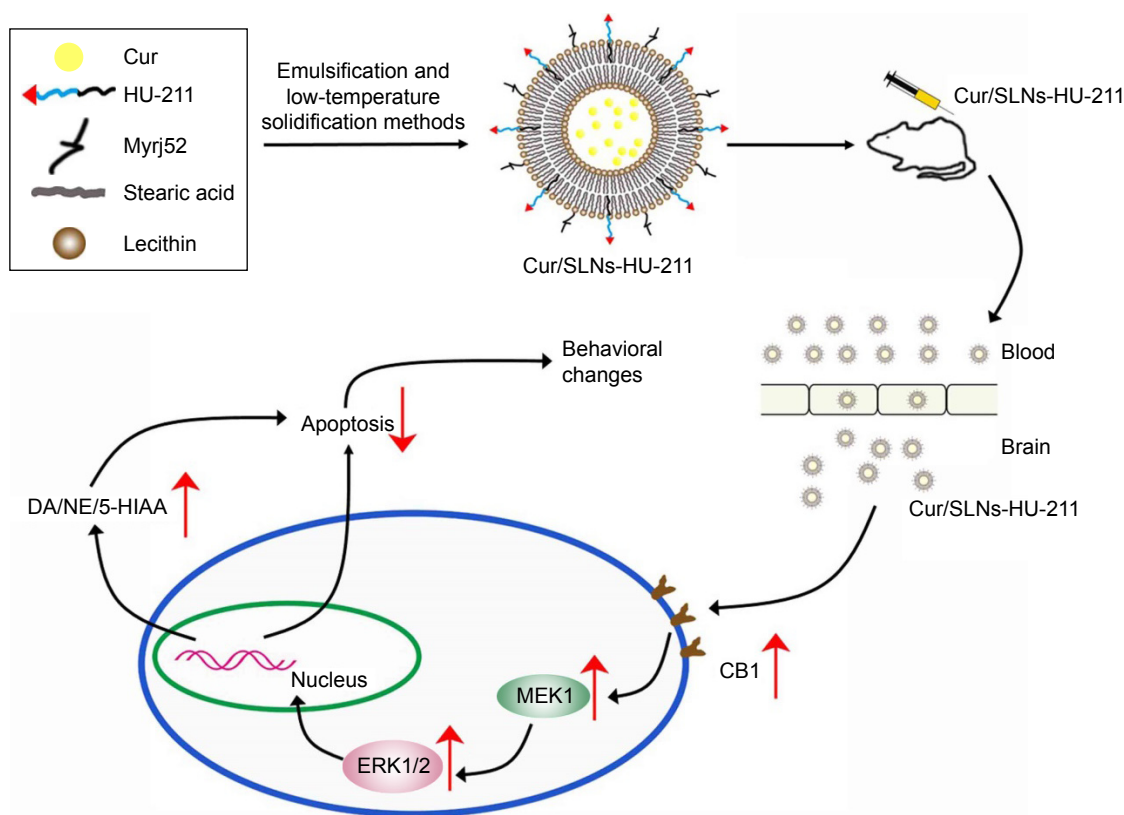


**Figure 10** Schematic representation of the mechanisms by which Cur/SLNs-HU-211 crosses the BBB for the CORT-induced major depression model.

**Notes:** After intraperitoneal injection of Cur/SLNs-HU-211 into the mice with major depression, the nanoparticles accumulated at brain. Then, Cur/SLNs-HU-211 upregulated the MEK1/ERK1/2 signaling pathways via activation of CB1 receptors, followed by an increased release of neurotransmitters (upward arrows) and a decrease of cell apoptosis (downward arrow).

**Abbreviations:** Cur, curcumin; Cur/SLNs-HU-211, curcumin and HU-211 coencapsulated solid lipid nanoparticles; CORT, corticosterone; BBB, blood-brain barrier; DA, dopamine.

antidepressant effects as compared to fluoxetine to some extent. Taken together, we propose that Cur/SLNs-HU-211 can be used as a promising antidepressant drug delivery system for CORT-induced depression.

## Conclusion

HU-211 and Cur coencapsulated SLNs (Cur/SLNs-HU-211) were successfully prepared by a modified emulsification and low-temperature solidification method. Cur/SLNs-HU-211 showed superior antidepressant activity compared to HU-211, Cur, and Cur/SLNs in vitro and in vivo. To sum up, the results of this study regarding Cur/SLNs-HU-211 provided a compelling argument for use of this approach in the treatment of major depression.

## Acknowledgments

This work was financially supported by the National Natural Science Foundation of China (Grant numbers 81301157, 31570849, and 81271694), International S&T Cooperation Program of China (Grant number 0102011DFA 32980), and the Fundamental Research Funds for the Central Universities.

## Disclosure

The authors report no conflicts of interest in this work.

## References

- Ferrari AJ, Somerville AJ, Baxter AJ, et al. Global variation in the prevalence and incidence of major depressive disorder: a systematic review of the epidemiological literature. *Psychol Med*. 2013;43(3):471–481.
- Nemeroff CB. The burden of severe depression: a review of diagnostic challenges and treatment alternatives. *J Psychiatric Res*. 2007;41(3–4):189–206.
- Leonard BE. The concept of depression as a dysfunction of the immune system. *Curr Immunol Rev*. 2010;6(3):205–212.
- Brasnjevic I, Steinbusch HW, Schmitz C, Martinez-Martinez P. Delivery of peptide and protein drugs over the blood-brain barrier. *Prog Neurobiol*. 2009;87(4):212–251.
- Nezafati MH, Vojdanparast M, Nezafati P. Antidepressants and cardiovascular adverse events: a narrative review. *ARYA Atheroscler*. 2015;11(5):295–304.
- Liu Y, Shen S, Li Z, et al. Cajaninstilbene acid protects corticosterone-induced injury in PC12 cells by inhibiting oxidative and endoplasmic reticulum stress-mediated apoptosis. *Neurochem Int*. 2014;78:43–52.
- Nakatani Y, Tsuji M, Amano T, et al. Neuroprotective effect of yokukansan against cytotoxicity induced by corticosterone on mouse hippocampal neurons. *Phytomedicine*. 2014;21(11):1458–1465.
- Workman JL, Gobinath AR, Kitay NF, Chow C, Brummelte S, Galea LA. Parity modifies the effects of fluoxetine and corticosterone on behavior, stress response and hippocampal neurogenesis. *Neuropharmacology*. 2016;105:443–453.
- Zhang HY, Zhao YN, Wang ZL, Huang YF. Chronic corticosterone exposure reduces hippocampal glycogen level and induces depression-like behavior in mice. *J Zhejiang Univ Sci B*. 2015;16(1):62–69.
- Zhao Y, Ma R, Shen J, Su H, Xing D, Du L. A mouse model of depression induced by repeated corticosterone injections. *Eur J Pharmacol*. 2008;581(1–2):113–120.
- Aggarwal BB, Harikumar KB. Potential therapeutic effects of curcumin, the anti-inflammatory agent, against neurodegenerative, cardiovascular, pulmonary, metabolic, autoimmune and neoplastic diseases. *Int J Biochem Cell Biol*. 2009;41(1):40–59.
- Mareshwari RK, Singh AK, Gaddipati J, Srimal RC. Multiple biological activities of curcumin: a short review. *Life Sci*. 2006;78(18):2081–2087.
- Zhu R, Wu X, Xiao Y, et al. Synergetic effect of SLN-curcumin and LDH-5-Fu on SMMC-7721 liver cancer cell line. *Cancer Biother Radiopharm*. 2013;28(8):579–587.
- Bhutani MK, Bishnoi M, Kulkarni SK. Anti-depressant like effect of curcumin and its combination with piperine in unpredictable chronic stress-induced behavioral, biochemical and neurochemical changes. *Pharmacol Biochem Behav*. 2009;92(1):39–43.
- Kulkarni SK, Bhutani MK, Bishnoi M. Antidepressant activity of curcumin: involvement of serotonin and dopamine system. *Psychopharmacology*. 2008;201(3):435–442.
- Yu ZF, Kong LD, Chen Y. Antidepressant activity of aqueous extracts of *Curcuma longa* in mice. *J Ethnopharmacol*. 2002;83(1–2):161–165.
- Darlington CL. Dexanabinol: a novel cannabinoid with neuroprotective properties. *IDrugs*. 2003;6(10):976–979.
- Juttler E, Potrovita I, Tarabin V, et al. The cannabinoid dexanabinol is an inhibitor of the nuclear factor-kappa B (NF-kappa B). *Neuropharmacology*. 2004;47(4):580–592.
- Maas AI, Murray G, Henney H 3rd, et al. Efficacy and safety of dexanabinol in severe traumatic brain injury: results of a phase III randomised, placebo-controlled, clinical trial. *Lancet Neurol*. 2006;5(1):38–45.
- Shohami E, Novikov M, Mechoulam R. A nonpsychotropic cannabinoid, HU-211, has cerebroprotective effects after closed head injury in the rat. *J Neurotrauma*. 1993;10(2):109–119.
- Burgos-Moron E, Calderon-Montano JM, Salvador J, Robles A, Lopez-Lazaro M. The dark side of curcumin. *Int J Cancer*. 2010;126(7):1771–1775.
- Jain SK, Gill MS, Pawar HS, Suresh S. Novel curcumin diclofenac conjugate enhanced curcumin bioavailability and efficacy in streptococcal cell wall-induced arthritis. *Indian J Pharm Sci*. 2014;76(5):415–422.
- Zhang ZY, Jiang M, Fang J, et al. Enhanced therapeutic potential of nano-curcumin against subarachnoid hemorrhage-induced blood-brain barrier disruption through inhibition of inflammatory response and oxidative stress. *Mol Neurobiol*. Epub December 26, 2015.
- Aggarwal N, Goindi S. Preparation and in vivo evaluation of solid lipid nanoparticles of griseofulvin for dermal use. *J Biomed Nanotechnol*. 2013;9(4):564–576.
- Neves AR, Queiroz JF, Weksler B, Romero IA, Couraud PO, Reis S. Solid lipid nanoparticles as a vehicle for brain-targeted drug delivery: two new strategies of functionalization with apolipoprotein E. *Nanotechnology*. 2015;26(49):495103.
- Singh I, Swami R, Pooja D, Jeengar MK, Khan W, Sistla R. Lactoferrin bioconjugated solid lipid nanoparticles: a new drug delivery system for potential brain targeting. *J Drug Target*. 2016;24(3):212–223.
- Yang X, Liu Y, Liu C, Zhang N. Biodegradable solid lipid nanoparticle flocculates for pulmonary delivery of insulin. *J Biomed Nanotechnol*. 2012;8(5):834–842.
- Wong HL, Chattopadhyay N, Wu XY, Bendayan R. Nanotechnology applications for improved delivery of antiretroviral drugs to the brain. *Adv Drug Del Rev*. 2010;62(4–5):503–517.
- Rempe R, Cramer S, Huwel S, Galla HJ. Transport of Poly(n-butylcyanoacrylate) nanoparticles across the blood-brain barrier in vitro and their influence on barrier integrity. *Biochem Biophys Res Commun*. 2011;406(1):64–69.
- Foger F, Hoyer H, Kafedjiiski K, Thaurer M, Bernkop-Schnurch A. In vivo comparison of various polymeric and low molecular mass inhibitors of intestinal P-glycoprotein. *Biomaterials*. 2006;27(34):5855–5860.
- Zhu S, Huang R, Hong M, et al. Effects of polyoxyethylene (40) stearate on the activity of P-glycoprotein and cytochrome P450. *Eur J Pharm Sci*. 2009;37(5):573–580.

32. Wang J, Zhu R, Gao B, et al. The enhanced immune response of hepatitis B virus DNA vaccine using SiO<sub>2</sub>@LDH nanoparticles as an adjuvant. *Biomaterials*. 2014;35(1):466–478.
33. Gregus A, Wintink AJ, Davis AC, Kalynchuk LE. Effect of repeated corticosterone injections and restraint stress on anxiety and depression-like behavior in male rats. *Behav Brain Res*. 2005;156(1):105–114.
34. Porsolt RD, Bertin A, Jalfre M. Behavioral despair in mice: a primary screening test for antidepressants. *Archives Internationales de Pharmacodynamie et de Therapie*. 1977;229(2):327–336.
35. Lee BH, Kim J, Lee RM, et al. Gintonin enhances performance of mice in rotarod test: Involvement of lysophosphatidic acid receptors and catecholamine release. *Neurosci Lett*. 2016;612:256–260.
36. Natu MV, de Sousa HC, Gil MH. Effects of drug solubility, state and loading on controlled release in bicomponent electrospun fibers. *Int J Pharm*. 2010;397(1–2):50–58.
37. Mohanty C, Sahoo SK. The in vitro stability and in vivo pharmacokinetics of curcumin prepared as an aqueous nanoparticulate formulation. *Biomaterials*. 2010;31(25):6597–6611.
38. Wu M, Zhang H, Zhou C, Jia H, Ma Z, Zou Z. Identification of the chemical constituents in aqueous extract of Zhi-Qiao and evaluation of its antidepressant effect. *Molecules*. 2015;20(4):6925–6940.
39. Wang J, Zhu R, Sun D, et al. Intracellular uptake of curcumin-loaded solid lipid nanoparticles exhibit anti-inflammatory activities superior to those of curcumin through the NF-kappaB signaling pathway. *J Biomed Nanotechnol*. 2015;11(3):403–415.
40. Dailly E, Chenu F, Renard CE, Bourin M. Dopamine, depression and antidepressants. *Fundam Clin Pharmacol*. 2004;18(6):601–607.
41. Hassanzadeh P, Hassanzadeh A. The CB(1) receptor-mediated endocannabinoid signaling and NGF: the novel targets of curcumin. *Neurochem Res*. 2012;37(5):1112–1120.
42. Kokona D, Themos K. Synthetic and endogenous cannabinoids protect retinal neurons from AMPA excitotoxicity in vivo, via activation of CB1 receptors: Involvement of PI3K/Akt and MEK/ERK signaling pathways. *Exp Eye Res*. 2015;136:45–58.
43. Colucci-D'Amato L, Perrone-Capano C, di Porzio U. Chronic activation of ERK and neurodegenerative diseases. *BioEssays*. 2003;25(11):1085–1095.
44. Gourley SL, Wu FJ, Taylor JR. Corticosterone regulates pERK1/2 map kinase in a chronic depression model. *Ann N Y Acad Sci*. 2008;1148:509–514.
45. Abbott NJ. Blood-brain barrier structure and function and the challenges for CNS drug delivery. *J Inherit Metab Dis*. 2013;36(3):437–449.
46. Allen TM, Cullis PR. Drug delivery systems: entering the mainstream. *Science*. 2004;303(5665):1818–1822.
47. Kulkarni SK, Dhir A. An overview of curcumin in neurological disorders. *Indian J Pharm Sci*. 2010;72(2):149–154.
48. Kulkarni S, Dhir A, Akula KK. Potentials of curcumin as an antidepressant. *ScientificWorldJournal*. 2009;9:1233–1241.
49. Vink R, Nimmo AJ. Multifunctional drugs for head injury. *Neurotherapeutics*. 2009;6(1):28–42.
50. Wang J, Wang H, Zhu R, Liu Q, Fei J, Wang S. Anti-inflammatory activity of curcumin-loaded solid lipid nanoparticles in IL-1beta transgenic mice subjected to the lipopolysaccharide-induced sepsis. *Biomaterials*. 2015;53:475–483.
51. Gastaldi L, Battaglia L, Peira E, et al. Solid lipid nanoparticles as vehicles of drugs to the brain: current state of the art. *Eur J Pharm Biopharm*. 2014;87(3):433–444.
52. Gershkovich P, Qadri B, Yacovan A, Amselem S, Hoffman A. Different impacts of intestinal lymphatic transport on the oral bioavailability of structurally similar synthetic lipophilic cannabinoids: dexanabinol and PRS-211,220. *Eur J Pharm Sci*. 2007;31(5):298–305.
53. Iqbal J, Hombach J, Matuszczak B, Bernkop-Schnurch A. Design and in vitro evaluation of a novel polymeric P-glycoprotein (P-gp) inhibitor. *J Control Release*. 2010;147(1):62–69.
54. Gao S, Li W, Zou W, et al. H2S protects PC12 cells against toxicity of corticosterone by modulation of BDNF-TrkB pathway. *Acta Biochimica et Biophysica Sinica*. 2015;47(11):915–924.
55. Sun XP, Shi Z, Pan RL, et al. Antidepressant-like effects and mechanism of action of SYG in depression model in rats. *Neuro Endocrinol Lett*. 2014;35(2):129–136.
56. Liu D, Wang Z, Gao Z, et al. Effects of curcumin on learning and memory deficits, BDNF, and ERK protein expression in rats exposed to chronic unpredictable stress. *Behav Brain Res*. 2014;271:116–121.
57. Witkin JM, Leucke S, Thompson LK, et al. Further evaluation of the neuropharmacological determinants of the antidepressant-like effects of curcumin. *CNS Neurol Disord Drug Targets*. 2013;12(4):498–505.
58. Xiong ZE, Dong WG, Wang BY, Tong QY, Li ZY. Curcumin attenuates chronic ethanol-induced liver injury by inhibition of oxidative stress via mitogen-activated protein kinase/nuclear factor E2-related factor 2 pathway in mice. *Pharmacogn Mag*. 2015;11(44):707–715.
59. Qui MS, Green SH. PC12 cell neuronal differentiation is associated with prolonged p21ras activity and consequent prolonged ERK activity. *Neuron*. 1992;9(4):705–717.
60. Roovers K, Assoian RK. Integrating the MAP kinase signal into the G1 phase cell cycle machinery. *BioEssays*. 2000;22(9):818–826.
61. Karanian DA, Brown QB, Makriyannis A, Bahr BA. Blocking cannabinoid activation of FAK and ERK1/2 compromises synaptic integrity in hippocampus. *Eur J Pharmacol*. 2005;508(1–3):47–56.
62. Miranti CK, Brugge JS. Sensing the environment: a historical perspective on integrin signal transduction. *Nat Cell Biol*. 2002;4(4):E83–E90.
63. Liu J, Qiao W, Yang Y, Ren L, Sun Y, Wang S. Antidepressant-like effect of the ethanolic extract from Suanzaorenhehuan Formula in mice models of depression. *J Ethnopharmacol*. 2012;141(1):257–264.
64. Kafa H, Wang JT, Rubio N, et al. Translocation of LRP1 targeted carbon nanotubes of different diameters across the blood-brain barrier in vitro and in vivo. *J Control Release*. 2016;225:217–229.

## International Journal of Nanomedicine

### Publish your work in this journal

The International Journal of Nanomedicine is an international, peer-reviewed journal focusing on the application of nanotechnology in diagnostics, therapeutics, and drug delivery systems throughout the biomedical field. This journal is indexed on PubMed Central, MedLine, CAS, SciSearch®, Current Contents®/Clinical Medicine,

Submit your manuscript here: <http://www.dovepress.com/international-journal-of-nanomedicine-journal>

Dovepress

Journal Citation Reports/Science Edition, EMBase, Scopus and the Elsevier Bibliographic databases. The manuscript management system is completely online and includes a very quick and fair peer-review system, which is all easy to use. Visit <http://www.dovepress.com/testimonials.php> to read real quotes from published authors.